

Growth of spatially ordered Ge nanoclusters in an amorphous matrix on rippled substratesM. Buljan,^{1,2} J. Grenzer,³ A. Keller,³ N. Radić,¹ V. Valeš,² S. Bernstorff,⁴ T. Cornelius,⁵ H. T. Metzger,⁵ and V. Holý²¹*Ruđer Bošković Institute, Bijenička cesta 54, 10000 Zagreb, Croatia*²*Charles University in Prague, 12116 Prague, Czech Republic*³*Forschungszentrum Dresden-Rossendorf, e.V., P.O. Box 510119, 01314 Dresden, Germany*⁴*Sincrotrone Trieste, 34102 Basovizza, Italy*⁵*European Synchrotron Radiation Facility (ESRF), BP 220, F-38043 Grenoble, France*

(Received 3 July 2010; published 14 September 2010)

So far, the growth of spatially ordered nanoclusters by multilayer deposition has been reported and explained satisfactorily only in crystalline materials. Here we demonstrate a method for the growth of spatially ordered nanoclusters in amorphous matrices, where the ordering is achieved in the single large domain. The regular ordering is induced by the deposition of a multilayer on a periodically rippled substrate at an elevated substrate temperature. During the deposition, the nanoclusters self-arrange, following the morphology of the substrate.

DOI: [10.1103/PhysRevB.82.125316](https://doi.org/10.1103/PhysRevB.82.125316)

PACS number(s): 68.35.bg, 61.05.cf, 68.55.-a

I. INTRODUCTION

Ordered nanocluster (NC) systems such as NC lattices or NC crystals are widely investigated nowadays due to their extraordinary properties¹⁻⁴ and many possible applications.⁵⁻⁷ The properties of NC systems can be manipulated by the sizes of NCs and their arrangement in the host matrix via confinement and collective behavior effects.⁸⁻¹¹ These effects are strongly influenced by the regularity of the geometrical arrangement of NCs since a regularity in ordering induces a uniformity of NC sizes and the collective properties of NCs can be observed only in very ordered systems.

Until recently, formation of regularly ordered NC arrays by a multilayer deposition was achieved only in crystalline systems.^{12,13} Our previous investigations show that the deposition of (Ge+SiO₂)/SiO₂ multilayers can result in a self-ordered growth of NCs also in amorphous matrix.^{10,11} However, so far the (Ge+SiO₂)/SiO₂ multilayers were deposited on a flat Si or glass substrate and consequently, only a short-range ordering of the NCs could be achieved; the ordered NC arrays appeared in small randomly oriented domains, each ordered domain consisting of only few NCs.

Here we demonstrate a deposition of an amorphous multilayer on a periodically corrugated (rippled) substrate, and show that the corrugation periodicity overcomes the above mentioned problem. In particular, we observe the formation of a three-dimensional (3D) NC lattice which appear in a single large domain. The arrangement of the NCs in the individual layers of the multilayer stack follows very well the geometry of the rippled substrate. Such possibility of formation of long-range ordered arrays of NCs could be important for semiconductor nanotechnology and optoelectronics, like in development of new lasers based on nanoclusters, in memory applications, in production of 3D photonics crystals, etc.

The main parameter of the substrate corrugation is the mean corrugation period L_{subs} ; in order to achieve the best efficiency of the corrugation, this period should be as close as possible to the “intrinsic” distance $\langle L \rangle$ of self-assembled NCs deposited on a flat surface. For the nominal Ge content

of 40% in the Ge+SiO₂ mixture and for the used deposition temperatures in the range between 500 and 700 °C this distance is approximately 15 nm.¹⁰ Such rippled substrate with typical period of 10–20 nm can be produced relatively simply on a large surface area by ion-beam erosion.¹⁴⁻¹⁶ Usual prepatterning methods such as electron-beam lithography cannot yield large surfaces with these extremely short ripple periods.¹⁷ We investigate the influence of the corrugation period on the mean in-plane distance of the NCs, and we compare the NC size distribution properties in the films grown simultaneously on rippled and on the flat substrates.

II. PREPARATION AND STRUCTURE OF SPATIALLY ORDERED Ge NANOCCLUSERS

Rippled substrates used for the deposition of (Ge+SiO₂)/SiO₂ multilayers were produced by ion-beam erosion which was performed at room temperature in a compact high vacuum chamber with a base pressure of 10⁻⁸ mbar with a Kaufman-type ion source, using Xe⁺ ions with the ion-beam incidence angle (with respect to the surface normal) of 67°, the energy of 1200 eV and the fluence of 2×10^{17} cm⁻².

Figures 1(a) and 1(b) show an atomic-force microscopy (AFM) image and grazing-incidence small-angle x-ray scattering (GISAXS) map, respectively, of a periodically corru-

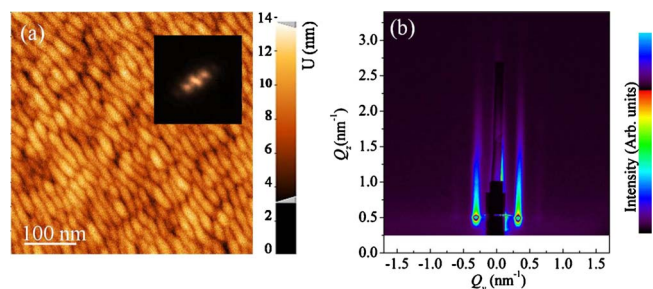


FIG. 1. (Color online) (a) The atomic-force microscopy picture of a rippled Si surface along with its Fourier transformation in the inset. (b) GISAXS intensity map of the rippled substrate.

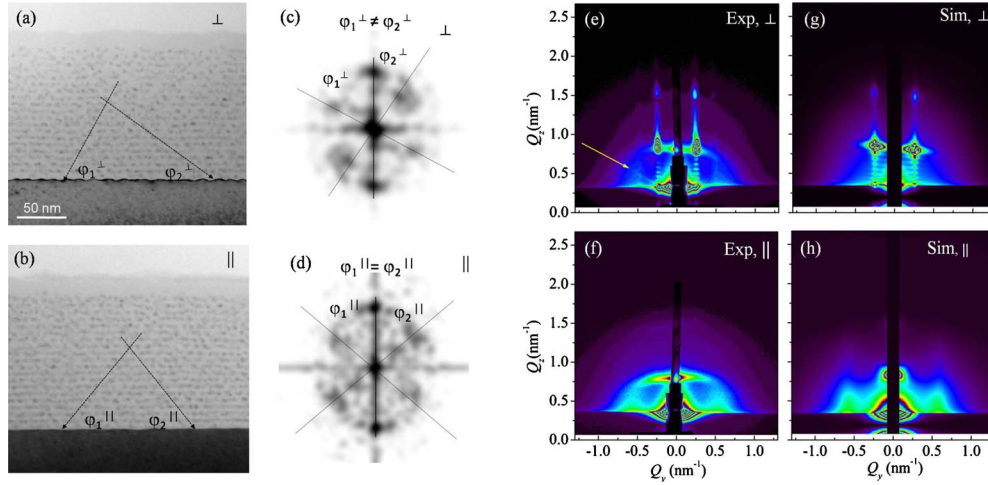


FIG. 2. (Color online) Structure of a $(\text{Ge}+\text{SiO}_2)/\text{SiO}_2$ multilayer deposited on a rippled Si substrate: (a) and (b) transmission electron micrographs of the cross sections of the multilayer taken in the directions across (denoted by \perp) and along (\parallel) the ripples, respectively. The arrows indicate the direction of the correlation of the positions of the NCs in different multilayer periods. (c) and (d) Fourier transformations of the TEM images. (e) and (f) GISAXS maps measured on the multilayer containing ten periods in \perp and \parallel configurations, respectively. The arrow indicates a streak coming from the facets of the ripples. (g) and (h) Simulations of the GISAXS intensity distributions shown in (e) and (f), respectively.

gated Si(111) surface obtained by the erosion. From the Fourier transformation (FT) of the AFM picture [inset of Fig. 1(a)] and from the positions of lateral sheets in GISAXS measurements we have determined the corrugation period of the substrates L_{subs} used for the depositions. The periods were slightly different for different substrates but all were in the range 17–23 nm. The GISAXS data used for the analysis of this system have been obtained at the synchrotron sources ESRF, Grenoble, ID01 beamline and Elettra, Trieste, SAXS beamline, using a photon energy of 11 keV and 8 keV, respectively, and two-dimensional (2D) photon detectors. The probing x-ray beam was set along the Q_x coordinate while the detector was placed in the $Q_y Q_z$ plane; the Q_z coordinate is perpendicular to the sample surface.

The films containing two, five, ten, and 20 $(\text{Ge}+\text{SiO}_2)/\text{SiO}_2$ periods were deposited simultaneously onto rippled and flat Si(111) substrates by magnetron sputtering, using the substrate temperature of 500 °C. We used argon at 0.66 Pa in a continuous flow (13 SCCM/min) as a working gas and pure Ge and pure SiO_2 targets in dc (6 W) and rf (125 W) magnetron operation modes, respectively. During the deposition of mixed $\text{Ge}+\text{SiO}_2$ layers the Ge: SiO_2 molar ratio of 40:60 was kept constant and the approximate thicknesses of $\text{Ge}+\text{SiO}_2$ and SiO_2 layers were 4 nm. After the deposition, the films were annealed in vacuum at 800 °C for 1 h.

As was shown in Refs. 10 and 11, the formation of spatially ordered Ge nanoclusters occurs during the deposition process. However, they consist of amorphous Ge and their shape is irregular and slightly elongated. Annealing treatment induces crystallization of the amorphous Ge nanoclusters and change in the nanocluster shape to spherical. The arrangement of the clusters remains approximately the same as before annealing.

Figures 2(a) and 2(b) show cross-section transmission-electron micrographs (TEMs) of the multilayer with 20 peri-

ods deposited onto a rippled surface after annealing. The micrographs shown in (a) and (b) are taken in the azimuths across (\perp) and along (\parallel) the ripples, respectively. The correlation of the NC positions at different interfaces (denoted “vertical correlation” here and indicated by dashed lines in Fig. 2) is visible in the whole depicted sample area showing that the NCs form a large three-dimensional NC lattice. The correlation angles (angles between the lines and the sample surface) are different for different cross sections indicating that indeed the NCs are ordered within one large domain, while for the case of deposition on the flat substrate, ordered regions appear only in small randomly oriented domains.¹⁰ The regular ordering of the NCs is better visible in the FTs of TEM images shown in the insets of Figs. 2(c) and 2(d) where distinct spots due to regular ordering are visible. From the FTs it follows that the NC positions in different layers in the multilayer stack are correlated in the directions inclined by $\phi_1^\perp = (63 \pm 1)^\circ$ and $\phi_2^\perp = (34 \pm 5)^\circ$ with the surface for the cross section made perpendicular to the ripples while both correlation angles are the same $\phi_1^\parallel = \phi_2^\parallel = (50 \pm 5)^\circ$ for the parallel cross section. The period of the ripples found from the TEM image was (16 ± 1) nm, the vertical period of the multilayer (T) was (8.3 ± 0.1) nm, while the lateral distance for the parallel cross section was (14 ± 1) nm. Very similar correlation angles can be found from the GISAXS maps measured on the ten period film, shown in Figs. 2(e) and 2(f), which provide structural data with an excellent statistics (about 10^{12} NCs in the illuminated volume). The average size of the NCs is found to be 2.3 nm with a very narrow size distribution.

We have fitted the measured GISAXS maps to simulations based on a modified paracrystal model,^{10,18} the simulated GISAXS maps are depicted in Figs. 2(g) and 2(h). Important parameters of the paracrystal model are the root-mean-square (rms) dispersions $\sigma_{LL,LV}$ expressing the quality of the NC ordering. The parameter σ_{LL} is the rms deviation

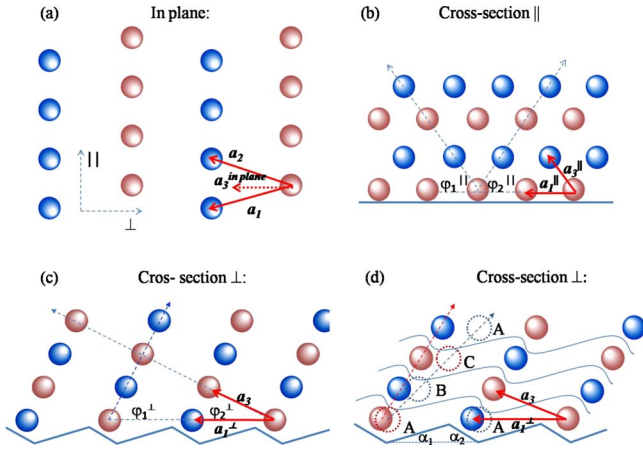


FIG. 3. (Color online) Schematic view of the arrangement of nanoclusters in the NC lattice formed on a rippled substrate. (a) In-plane view, direction \parallel is set along the ripples; the projection of \mathbf{a}_3 on the sample surface is shown by dashed arrow. To improve visualization, the NCs are shown by alternating rows of dark and light (blue and red online) spheres, directioned along the ripples. (b) and (c) Cross-sectional view showing projections of the positions of the NCs in directions parallel and perpendicular to the ripples direction, respectively. (d) Influence of the ripples morphology on the NC stacking. The asymmetric shape of the ripples described by the angles $\alpha_{1,2}$ of the ripple facets with the mean surface ($\alpha_1 \neq \alpha_2$) causes stacking of NCs different from the expected $ABCABC$ stacking. The fcc-like $ABCABC$ stacking is indicated by dashed circles.

in the lateral distances between neighboring NCs at the same interface and σ_{LV} denotes the rms deviation of the relative lateral positions of two neighboring NCs at two subsequent interfaces lying in the ordering direction, i.e., along the arrows in Figs. 2(a) and 2(b) (see Ref. 10 for more details). Therefore, the parameter σ_{LL} characterizes the quality of the lateral NC ordering while σ_{LV} expresses the quality of the “inheritance” of the NC positions across the multilayer stack. The values of σ_{LL}^{\perp} and σ_{LV}^{\perp} were found to be $(19 \pm 2)\%$ and $(27 \pm 2)\%$ of the length of the basis vector \mathbf{a}_1 (see Sec. III), respectively, for the ten period film, and they were slightly increasing with the number of the deposited layers. The value of σ_{LL}^{\parallel} was found to be $30 \pm 2\%$. Thus, the better ordering is achieved in direction perpendicular to the ripples direction. This result is expectable since the ordering in that direction is determined by the ripples periodicity. More freedom in the NC ordering exists in direction along the ripples, what results with larger rms deviation of the in-plane NC positions. For the case of the flat substrate σ_{LL}^{\perp} were $31 \pm 2\%$ while σ_{LV}^{\perp} were $27 \pm 2\%$ of the basis vector length.¹⁰

III. MODEL OF THE ORDERING OF NANOCCLUSERS

The paracrystal model of the arrangement of the NCs used for the fitting was deduced from TEM and GISAXS data and is shown in Fig. 3. In the plane parallel to the substrate [see Fig. 3(a)] the NCs are ordered in a disordered 2D hexagonal lattice defined by mean basis vectors \mathbf{a}_1 and \mathbf{a}_2 , where the absolute values of these vectors might be different. The ripple period L_{subs} equals the component of $\mathbf{a}_{1,2}$

perpendicular to the ripples, i.e., $a_{1,2}^{\perp} = L_{\text{subs}}$. The lateral disorder of the NCs is expressed by the parameter σ_{LL} . As was found by GISAXS analysis the lateral disorder is larger for direction parallel to the ripples. That means the hexagonal lattice is more distorted in that direction, i.e., the rows of NCs along the ripples (see Fig. 3) might be more mutually shifted in the \parallel direction.

The 2D arrays are stacked in vertical direction along the third basis vector \mathbf{a}_3 , lateral deviations from this direction are described by σ_{LV} . The cross-sectional views of the NC lattice structure in direction \perp and \parallel to the ripples are shown in Figs. 3(b) and 3(c). It is worthy to note that the experimentally observed arrangement of the NCs is not exactly the same as the expected $ABCABC$ layer stacking. The theoretical values of the angles $\varphi_{1,2}^{\perp,\parallel}$ for $ABCABC$ stacking are

$$\varphi_{1\text{theor}}^{\perp} = \arctan(3T/L_{\text{subs}}),$$

$$\varphi_{2\text{theor}}^{\perp} = \arctan(3T/L_{\text{subs}}/2),$$

$$\varphi_{1,2\text{theor}}^{\parallel} = \arctan(2T/a_1^{\parallel}).$$

Using the values of ripple period and the multilayer period found from the TEM pictures and the above formulas for $\varphi_{1,2}$ we obtained $\varphi_{1\text{theor}}^{\perp} = (57.3 \pm 0.6)^{\circ}$, $\varphi_{2\text{theor}}^{\perp} = (38 \pm 3)^{\circ}$, and $\varphi_{1,2\text{theor}}^{\parallel} = (50 \pm 5)^{\circ}$ while the angles determined directly from TEM are $\varphi_1^{\perp} = (63 \pm 1)^{\circ}$, $\varphi_2^{\perp} = (34 \pm 5)^{\circ}$, and $\varphi_{1,2}^{\parallel} = (50 \pm 5)^{\circ}$. The comparison of theoretical and experimentally obtained angles shows that φ_1^{\perp} is always larger than the theoretical value while the value of φ_2^{\perp} is smaller. Both angles obtained for the \parallel configuration are approximately the same as the theoretical ones. The correlation angles were determined from the GISAXS maps as well. We have examined films with two, five, and ten vertical periods and films deposited on substrates with slightly different rippled periods in the range 17–23 nm. In all cases, the angle φ_1^{\perp} was larger than the corresponding $ABCABC$ stacking angle, φ_2^{\perp} was always smaller, while angles $\varphi_{1,2}^{\parallel}$ were the same. The GISAXS intensity distribution is very sensitive to the value of the correlation angles and it was impossible to obtain a GISAXS simulation similar to the experimentally measured if the exact $ABCABC$ stacking was used.

We explain the difference between the measured values of the correlation angles $\varphi_{1,2}^{\perp,\parallel}$ and the values following from the $ABCABC$ stacking by the influence of the morphology of individual ripples on the ordering of NCs, this is schematically shown in Fig. 3(d). The explanation is based on the effect of the local morphology of the growing surface on the surface diffusion of deposited adatoms, which is thoroughly explained in our previous paper.¹⁰ The Ge nanoclusters nucleate during the growth in local minima of the chemical potential $\mu(s)$ of deposited adatoms that move along the growing surface by two-dimensional surface diffusion (s is the coordinate along the surface). Since the deposited material is fully amorphous, μ is determined only by the local curvature $\kappa(s)$ of the surface and by the local surface energy density $\gamma(s)$,

$$\mu(s) = \text{const} + \kappa(s)\gamma(s)V_0,$$

where V_0 is the atomic volume. The morphology of the growing surface that influences the local curvature κ depends on the position of the nanoclusters in the previous layer buried below the growing surface. The ripples formed by ion-beam sputtering have an asymmetric cross section so that the local profile of $\kappa(s)$ is asymmetric, too. Therefore the NCs do not nucleate in the centers between two neighboring ripples (as would be the case for exact *ABCABC* stacking) but closer to the more inclined ripple facet.^{19,20} The position of the NCs is then replicated to the layers above and causes a deviation of the correlation angles $\varphi_{1,2}$ from the expected *ABCABC* value. Namely, the correlation angle φ_2^\perp is always smaller than the corresponding angle for *ABCABC* stacking, while φ_1^\perp is larger, what is exactly observed in the experimental data. Such rearrangement does not affect the angles in \parallel configuration.

The mentioned growth type is crucial for the formation of the single domain with the regularly ordered NCs. If the stacking of NCs would follow *ABCABC* stacking, the NCs in the first layer should nucleate along the lines crossing the centers between two neighboring ripples. Such initial arrangement would cause two *equivalent* positions of the NCs in the second layer, i.e., two possible equivalent \mathbf{a}_3 vectors would appear. Such a NC arrangement would give rise to symmetrical FTs of the TEM images and symmetrical GISAXS intensity maps, what is not found experimentally.

IV. INFLUENCE OF THE SELF-ASSEMBLY ON THE NANOCCLUSERS SIZE DISTRIBUTION

Finally we examine the dependence of the size distribution of the NCs on the growth type. Figure 4 shows the size distributions found for the five period multilayers grown at 500 °C on rippled and flat substrates (in both cases the self-ordering effect was active) and the size distribution that resulted from the growth at room temperature, at which no self-ordering occurred (all multilayers were annealed after the deposition). From Fig. 4 it is clear that the growth on a rippled substrate produces the narrowest size distribution of NCs while the broadest distribution is obtained for the non-correlated growth (realized by the deposition on a flat substrate at room temperature). Such behavior is expected since the size distribution of NCs depends on the distribution of the distances of NCs. As it was shown by GISAXS analysis and discussed above, the NC lattice formed by the self-ordering growth on the rippled substrate has smaller rms dis-

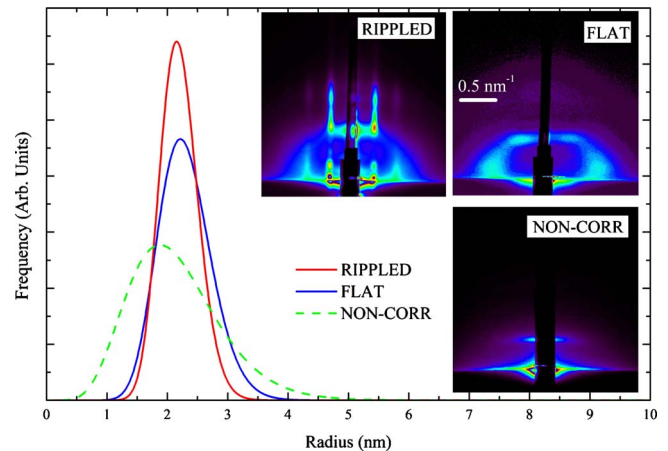


FIG. 4. (Color online) Size distribution of the nanoclusters obtained for different growth types. The self-ordering growth is performed on the rippled (red line) and flat (blue line) substrate at 500 °C while noncorrelated growth (green line) is realized at room temperature on the flat substrate. The insets show the GISAXS maps from which the size distributions were calculated.

persions $\sigma_{LL,LV}^{\perp,\parallel}$ than the corresponding NC lattice formed on the flat substrate. The highest rms dispersions $\sigma_{LL,LV}^{\perp,\parallel} = 0.6|a_1|$ occur for the noncorrelated growth type what is in agreement with the obtained results.

V. SUMMARY

In summary we have demonstrated that quasiperiodic ripples on Si substrate induce ordering of the positions of Ge nanoclusters in subsequently deposited (Ge+SiO₂)/SiO₂ multilayers. We have discussed the physical reasons for this ordering mechanism and we have demonstrated the dependence of the dispersion of the size distribution of the NCs on the degree of the ordering of their positions.

ACKNOWLEDGMENTS

The authors are grateful to Aleksa Pavlešin for assistance during the sample preparation. Transmission electron micrographs were kindly provided by A. Mücklich. M.B. acknowledges support from the National Foundation for Science, Higher Education and Technological Development of the Republic Croatia, M.B. and V.H. acknowledge the support from the Ministry of Education of Czech Republic (Project No. MSM 0021620834) and by the EC (Project No. 214499 NAMASTE).

¹A. P. Alivisatos, *Science* **271**, 933 (1996).

²C. Bostedt, T. van Buuren, T. M. Willey, N. Franco, and L. J. Terminello, *Appl. Phys. Lett.* **84**, 4056 (2004).

³S. K. Ray, *Opt. Mater.* **27**, 948 (2005).

⁴A. Dowd, R. G. Elliman, M. Samoc, and B. A. Luther-Davies, *Appl. Phys. Lett.* **74**, 239 (1999).

⁵T. C. Chang, *Electrochem. Solid-State Lett.* **7**, G17 (2004).

⁶J. Konle, H. Presting, H. Kibbel, K. Thinke, and R. Sauer, *Solid-State Electron.* **45**, 1921 (2001).

⁷U. V. Desnica, M. Buljan, P. Dubček, Z. Sikatić, I. Bogdanović-Radović, S. Bernstorff, U. Serincan, and R. Turan, *Nucl. Instrum. Methods Phys. Res. B* **249**, 843 (2006).

- ⁸A. Courty, A. Mermet, P. A. Alboy, E. Duval, and M. P. Pileni, *Nature Mater.* **4**, 395 (2005).
- ⁹D. Grützmacher, T. Fromherz, C. Dais, J. Stangl, E. Müller, Y. Ekinci, H. H. Solak, H. Sigg, R. T. Lechner, E. Wintersberger, S. Birner, V. Holý, and G. Bauer, *Nano Lett.* **7**, 3150 (2007).
- ¹⁰M. Buljan, U. V. Desnica, M. Ivanda, N. Radić, P. Dubček, G. Dražić, K. Salamon, S. Bernstorff, and V. Holý, *Phys. Rev. B* **79**, 035310 (2009).
- ¹¹M. Buljan, U. V. Desnica, G. Dražić, M. Ivanda, N. Radić, P. Dubček, K. Salamon, S. Bernstorff, and V. Holý, *Nanotechnology* **20**, 085612 (2009).
- ¹²G. Springholz, V. Holý, M. Pinczolits, and G. Bauer, *Science* **282**, 734 (1998).
- ¹³V. Holý, J. Stangl, T. Fromherz, R. T. Lechner, E. Wintersberger, G. Bauer, C. Dais, E. Muller, and D. Grutzmacher, *Phys. Rev. B* **79**, 035324 (2009).
- ¹⁴W. L. Chan and E. Chason, *J. Appl. Phys.* **101**, 121301 (2007).
- ¹⁵A. Keller, R. Cuerno, S. Facsko, and W. Moller, *Phys. Rev. B* **79**, 115437 (2009).
- ¹⁶A. Biermanns, U. Pietsch, J. Grenzer, A. Hanisch, S. Facsko, G. Carbone, and T. H. Metzger, *J. Appl. Phys.* **104**, 044312 (2008).
- ¹⁷J. Stangl, V. Holý, and G. Bauer, *Rev. Mod. Phys.* **76**, 725 (2004).
- ¹⁸M. Buljan, G. Dražić, N. Radić, S. Bernstorff, and V. Holý (unpublished).
- ¹⁹S. Camelio, D. Babonneau, D. Lantiat, L. Simonot, and F. Pailoux, *Phys. Rev. B* **80**, 155434 (2009).
- ²⁰U. Pietsch, V. Holý, and T. Baumbach, *High-Resolution X-Ray Scattering* (Springer-Verlag, New York, 2004).